APS European Society for Paediatric Research Society for Pediatric Research

SPECIAL ARTICLE

Novel insights into residual hematopoiesis from stem cell populations in pediatric B-acute lymphoblastic leukemia

Erivan Demanou-Peylin[1,2,9], Sarah Blanc[1,2,9], Thomas Da Costa Pereira[3,4], Véronique Parietti[5], Benjamin Saintpierre[6,7], Franck Letourneur[6,7], Michèle Souyri[3,4] and Carine Domenech[1,2,8]✉

Pediatric Research (2022) 91:1064–1068; https://doi.org/10.1038/s41390-021-01885-w

Hematopoiesis is a complex process that ensures production of highly specialized blood cells, emerging from bone marrow (BM) every day.[1] This continuous blood cell production is finely regulated by a molecular network of intrinsic and microenvironmental signals that control a rare pool of multipotent hematopoietic stem cells (HSCs), niched in the BM, which stands at the top of the hematopoietic hierarchy organization. During malignant hematological disorders, including acute leukemias (AL), oncogenic event(s) change(s) the key regulator of pathological hematopoietic cells (more or less differentiated) and give(s) them a capacity for unlimited self-renewal, by reversing normal proliferation control, blocking cell differentiation, and promoting resistance to apoptosis.[2] Contrary to adult AL, 80% of pediatric AL are developed from lymphoid lineage (ALL). The uncontrolled proliferation of these malignant progenitors primarily affects B cells (80%) and supports tumor growth at the expense of normal blood cell production with an often-massive BM invasion with more than 90% of lymphoblasts.[3] As a result, malignant niche outcompetes native hematopoietic stem and progenitor cells (HSPCs) niche by the mobilization of $CD34^+$ cells, hence disrupting normal HSC and progenitor functions.[4–6] Today, the status of residual naive HSPC populations in the BM at initial diagnosis or relapse in pediatric B-ALL is still poorly investigated. In this work we show that a residual hematopoiesis is still present in many patients, even when BM is fully invaded, and presents different properties depending on the B-ALL status (initial diagnosis or relapse), with residual hematopoiesis from relapsed patients being in a better shape than residual hematopoiesis from patients at initial diagnosis.

We first sorted a large panel of medullary mononuclear cells (MMC) from pediatric B-ALL patients ($n = 30$), including 25 initial diagnosis and 5 relapses (Table 1). BM samples from children and adolescents without malignant hemopathies ($n = 4$) were used as control (Ct). $CD34^+CD38^-$ HSPCs (or $CD34^+$ when no $CD38^-$ fraction could be detected—indicated by + in Table 1) were sorted from MMC isolated on Ficoll-Hypaque gradient (Pancoll, PAN Biotech GmbH). As B-ALL BM are massively invaded by leukemic blasts, we needed to use a very stringent protocol of cell sorting to isolate residual HSPCs free of any blast contamination: as shown in Fig. 1a, after isolation of $CD45^+$ cells, $CD19^-$ and $CD10^-$ cell populations were selected to eliminate leukemic blasts. Residual $CD34^+CD38^-$ HSPCs were sorted from this $CD45^+CD19^-CD10^-$ population.

Next, we co-cultured these residual HSPCs during 14 days with murine MS-5 cells in myelo-lymphoid conditions as described by Hussein et al.[7] Cells present in the supernatant were analyzed by flow cytometry to evaluate hematopoietic production and lympho-myeloid differentiation. Despite the fact that the number of sorted HSPCs was lower in relapse patients than patients at initial diagnosis (mean: 47 cells vs 230 cells, p: 0.01) (Fig. 1b), their hematopoietic production assessed by the ratio of the total number of live $CD45^+$ cells obtained after 14 days of culture to the input number of sorted HSPCs was much better (mean 6.7 vs 0.6 for patients at initial diagnosis), and comparable to the hematopoietic production obtained with HSPCs sorted from control pediatric BM (mean 5.9) (p: 0.0001) (Fig. 1c). Interestingly, only 31.8% of CD45 cells were still alive after 14 days of cocultures with HSPCs from initial diagnosis, compared to 72.7 and 77.8% for HSPCs from relapsed and controls, respectively (p: 0.002) (Fig. 1d). No difference was observed between patients with good or poor prognosis factors (data not shown). Altogether, these results indicate that residual HSPCs present in the BM of relapsed patients are in better conditions than residual HSPCs in the BM of patients at initial diagnosis. Analysis of myeloid and lymphoid content did not show any significant difference between B-ALL (initial diagnosis or relapse) and Ct.

No HSPC could be sorted for 3 out of the 25 initial B-ALL patients (Patient #13, #18, and #22—Table 1). Taking advantage of the PDX NSG model,[8] we were able to amplify BM cells from Patient #13 and Patient # 22 after intravenous injection of initial BM cells into irradiated (1.25 Gy) adult or intra-hepatic injection into newborn NSG mice, respectively. We also amplified cells from Patient #3 and from control Patient #33. $CD19^+$ blast cells sorted from the BM or the spleen of NSG mice had the same phenotypic characteristics as initial CD19+ blast cells from patients (not shown). In addition, $CD34^+CD38^-$ cells could be sorted, which indicates that even if in a bad shape, initial medullary residual HSPCs have also been able to amplify in the NSG context. These HSPCs were tested in co-culture, like initial medullary HSPCs. As shown in Fig. 1d, a low ratio of the total number of live $CD45^+$ cells obtained to the input number of sorted HSPCs residual

[1]Institut d'Hématologie et d'Oncologie Pédiatrique, Hospices Civils de Lyon, Université-Lyon1, Lyon, France. [2]Laboratoire Apoptose, Cancer and Développement, Centre de Recherche en Cancérologie de Lyon, INSERM U1052-CNRS UMR5286, Lyon, France. [3]Université de Paris, Institut de Recherche Saint-Louis (IRSL), Paris, France. [4]Institut National de la Santé et de la Recherche Médicale (INSERM) Unité 1131, Paris, France. [5]Département d'expérimentation animale, Université de Paris, IRSL, Paris, France. [6]Genom'IC, Hôpital Cochin, Université de Paris, Paris, France. [7]Institut National de la Santé et de la Recherche Médicale (INSERM) Unité 1016, Paris, France. [8]Faculté de médecine et de maïeutique Lyon Sud, Université Lyon 1, Lyon, France. [9]These authors contributed equally: Erivan Demanou-Peylin, Sarah Blanc. ✉email: carine.halfondomenech@ihope.fr

Received: 22 September 2021 Accepted: 19 November 2021
Published online: 9 December 2021

Table 1. Clinical and biological characteristics of B-ALL and control patients.

Patient number	Age (years)	Sex	Medullary sample	Blasts invasion	Cytogenetic	Molecular biology
1	2	M	Initial B-ALL	60	t (12; 21)	ETV6 RUNX1
2	3	F	Initial B-ALL	90	t (12; 21)	ETV6 RUNX1
3[a]	4	F	Initial B-ALL	85	t (12; 21)	ETV6 RUNX1
4	6	M	Initial B-ALL	70	t (12; 21)	ETV6 RUNX1
5	17	M	Initial B-ALL	85	t (12; 21)	ETV6 RUNX1
6[b]	2	F	Initial B-ALL	90	Hyperdiploidy (57ch)	
7[b]	6	M	Initial B-ALL	60	Hyperdiploidy (56 ch)	
8[b]	7	M	Initial B-ALL	75	Hyperdiploidy (55ch)	
9	8	M	Initial B-ALL	90	Hyperdiploidy (52ch)	
10	18	M	Initial B-ALL	90	Hyperdiploidy (54ch)	
11	1	M	Initial B-ALL /pro-B	55	t (1; 19)	TCF3
12	8	F	Initial B-ALL /pro-B	85	t (4; 11)	KMT2A rearrangement
13[a,c]	10	F	Initial B-ALL /pro-B	85	t (4; 11)	KMT2A rearrangement
14	9	F	Initial B-ALL/pro-B	75	46XX	
15[b]	1	M	Initial B-ALL	85	46XY	
16	11	F	Initial B-ALL	90	46XX	IKZF1/ERG/VPREB1 deletion
17	17	F	Initial B-ALL	85	46XX	KRAS mutation
18[c]	2.5	M	Initial B-ALL	80	Complex karyotype	IKZF1 deletion/transcript ZMIZ1-ABL1 (phi like)
19	4	M	Initial B-ALL	90	t (9; 22)	BCR abelson transcript/IKZF1 deletion
20	5	M	Initial B-ALL	90	t (9; 22) Monosomy 7	BCR abelson transcript
21[b]	10	M	Initial B-ALL	85	Hypodiploidy (37ch) Monosomy 7	P53 mutation
22[a,c]	12	M	Initial B-ALL	85	ampl ch 21	amp AML1
23	15	F	Initial B-ALL	85	ampl ch 21	ampl AML1
24	18	M	Initial B-ALL	80	Complex karyotype	IKZF1 deletion
25	18	M	Initial B-ALL	90	46XY	IKZF deletion/transcript ZC3HAV1-ABL2 (phi like)
26	14	M	Relapse B-ALL	80%	Hyperdiploidy (53 ch)	
27	4	F	Relapse B-ALL	10%	46XX	
28	11	M	Relapse B-ALL	10%	46XY	
29	4	F	Relapse B-ALL	80%	Complex karyotype	Amp PAX5, del CDKN 2A, del CDKN2B
30	24	F	Relapse B-ALL	60%	t (1; 19)	
31	2	M	Ct			
32	2	M	Ct			
33[a]	4	M	Ct			
34	2	F	Ct			

Bone marrow samples were collected from B-ALL patients at initial diagnosis or at relapse and from control patients after informed consent according to institutional guidelines and the ethics committee of the Hospices Civils de Lyon (Clinicaltrials.gov NCT03278145). Initial: B-ALL patient detected at initial diagnosis; Relapse: B-ALL patient diagnosed at relapse; pro-B B-ALL: leukemia stopped at an early stage of differentiation, expressing the CD19 but not the CD10. *F* female, *M* male, *Ct* control patients, *ch* chromosomes, *t* translocation, *amp* amplification, *del* deletion. [a]Patients injected in PDX models. [b]CD34-positive sorted cells. [c]No sorted HSPC.

hematopoiesis was also found for Patients #13 and #22, as expected for B-ALL at initial diagnosis. Ratio observed for PDX-HSPCs sorted from Patient #3 and control Patient #33 were similar to the ratio obtained from initial medullary HSPCs sorted from these patients.

Residual HSPCs from relapse B-ALL patients (isolated or combined medullary relapses) demonstrated properties closer to Ct HSPCs, contrasting to residual HSPCs from B-ALL at initial diagnosis. Interestingly, principal component analysis (PCA) of RNA sequencing of $CD19^+$ blast cells from these patients ($n = 32$) and $CD19^+$ cells from control pediatric BM also showed that out of the six relapse B-ALL studied, four were found in the Ct group cluster (patients #27, #28, #29 and #30—Fig. 2a). Among these four patients, two had a combined relapse (ophthalmic and BM), with less than 10% blasts in their BM (Patients #27 and #28), while two had an isolated BM relapse with 60 and 80% blasts (Patients #30 and #29, respectively). Analysis of the contrast between RNA content from these four relapsed B-ALL and from Ct demonstrated

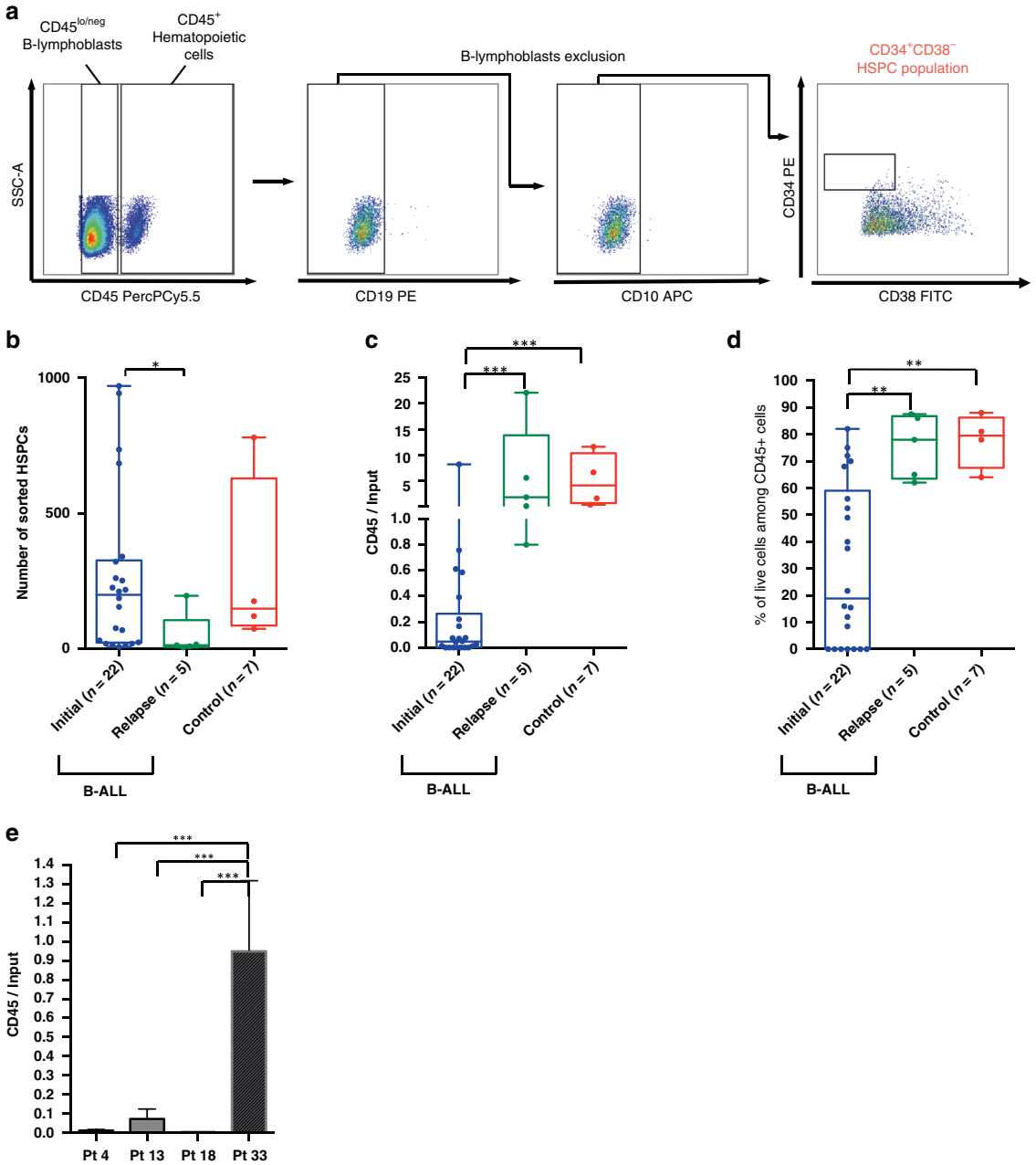

Fig. 1 Residual HSPCs sorted from relapse B-ALL BM give rise to a better hematopoietic production than residual HSPCs from B-ALL BM at initial diagnosis. a Gating strategy for $CD34^+CD38^-$ HSPC sorting: 1. $CD45^{lo/neg}$ blast exclusion by gating on $CD45^+$ population, and selecting $CD19^-$ and $CD10^-$ cells; 2. $CD34^+CD38^-$ HSPCs sorting. **b** Total number of HSPCs sorted from patients BM MNCs. **c** Hematopoietic production of sorted residual HSPCs from primary patients BM or **e** after amplification in the NSG PDX model, after co-culture on MS5 stromal support during 14 days in the presence of 10 ng/ml of SCF, IL-7, IL-2, IL-3, and TPO.[7] Hematopoietic production was assessed by the ratio of the number of total live $CD45^+$ cells present in the supernatant of the culture to the input number of sorted HSPCs. **d** Percentage of live CD45+ cells produced by HSPCs from initial diagnosis after 14 days of cocultures, compared to CD45+ cells produced by HSPCs from relapse and controls. The asterisks indicate statistical significance based on nonparametric Kruskal–Wallis and two-sided Wilcoxon–Mann–Whitney tests calculated with GraphPad Prism 9 (GraphPad Software Inc.) *p: 0.01; **p: 0.002; ***$p < 0.001$. Initial diagnosis: B-ALL patient detected at initial diagnosis; Relapse: B-ALL patient diagnosed at relapse. *Ct* control patients, *Pt* patient, *B-ALL* B-acute lymphoblastic leukemia.

only 159 differentially expressed genes (DEG) (adjusted p value <0.05), with 82 up- and 77 down-regulated (fold-change >1.5 or < −1.5). Gene ontology (GO) enrichment analysis, performed using DAVID (database used for annotation, visualization, and integrated discovery),[9] indicated that the main biological process (BP) down-regulated in $CD19^+$ blasts from relapsed B-ALL is involved in regulation of immune response while up-regulated BP encompass positive regulation of cell cycle, and apoptotic signaling in response to DNA damage (Fig. 2b). Contrast between RNA content from B-ALL patients at initial diagnosis and control demonstrated much more DEG (4481), with 2473 up- and 1724 down-regulated, with main down-regulated BP implicated in apoptotic process and immune response, and up-regulated BP involved in epigenetic regulation of gene expression and in cell adhesion.

In summary, our study demonstrates for the first time that a residual hematopoiesis is still present in many patients at diagnosis of B-ALL. However, our results indicate that the few sorted residual HSPCs present a poor ability to produce

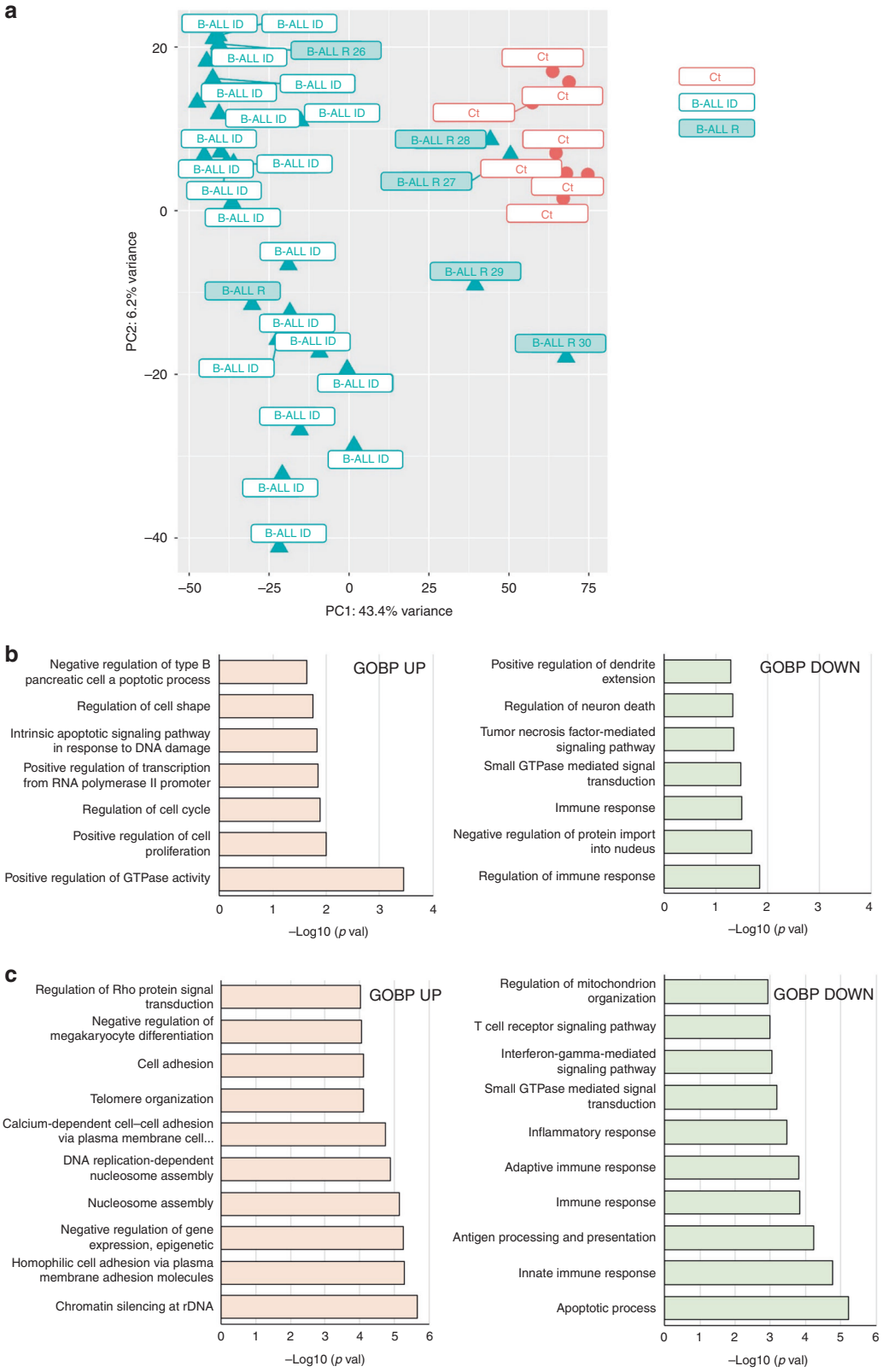

hematopoietic cells, with a high mortality rate (Fig. 1c, d), which can be explained by their low intrinsic functional activity. Indeed, culture of these HSPCs in vitro in a stable microenvironment able to support normal hematopoiesis, in the presence of cytokines revealed a low hematopoietic differentiation burden. In contrast, residual hematopoiesis of relapsed patients is in a better shape, closer to the hematopoiesis of control pediatric BM, even in the context of a major BM invasion (≥60%). These results were quite surprising because relapses are sign of aggressiveness of the disease. Actually, transcriptomic analysis of $CD19^{+}$ B-lymphoblast

Fig. 2 RNA content from relapse B-ALL CD19+ blasts cells is closer to RNA content of control CD19+ cells than that of B-ALL CD19+ at initial diagnosis. a Principal component analysis (PCA) of the top 500 most variable genes from RNA content of sorted relapse B-ALL $CD19^+$ blasts cells (blue triangles, and indicated with R and a number on the label), B-ALL $CD19^+$ blasts at initial diagnosis (blue triangles) and control $CD19^+$ cells (red circles). **b** Enriched GO biological process (BP) terms for up- (left panel) and down- (right panel) regulated genes in the $CD19^+$ blasts from the four relapse B-ALL patients whose RNA content clusterize with that of control $CD19^+$ cells, contrasted with control $CD19^+$ cells RNA. GO enrichment analysis was performed using DAVID (database used for annotation, visualization, and integrated discovery).[9] GO BP as –Log10 (*p* value). **c** Enriched GO biological process (BP) terms for up- (left panel) and down- (right panel) regulated genes in the $CD19^+$ blasts from B-ALL patients at initial diagnosis, contrasted with of control $CD19^+$ cells RNA. B-ALL ID patient detected at initial diagnosis, B-ALL R patient diagnosed at relapse, Ct control patients, B-ALL B-acute lymphoblastic leukemia, GO BP Gene ontology biological pathway.

cells of four out of six relapse patients also indicated that their RNA content is close to that of control B-lymphoid $CD19^+$ cells.

B-lymphoblastic invasion of pediatric BM results in a negative impact on the functionality of resident HSPCs and microenvironment.[10] As a result, at diagnosis normal residual hematopoiesis is very weak. By killing B-lymphoblasts, chemotherapy allows BM microenvironment to resume its supportive role and the few residual HSPCs to function again during remission. Our original results indicate for the first time that when the relapse occurs residual HSPCs might have gained a better ability to self-renew and to differentiate in an adverse environment, and can behave normally, at least for a while.

REFERENCES

1. Kaushansky, K. Lineage-specific hematopoietic growth factors. *N. Engl. J. Med*. **354**, 2034–2045 (2006).
2. Pui, C. H., Relling, M. V. & Downing, J. R. Acute lymphoblastic leukemia. *N. Engl. J. Med*. **350**, 1535–1548 (2004).
3. Domenech, C. Leucémies aiguës lymphoblastiques de l'enfant et de l'adolescent. *EM-Consulte*. 0.1016/S1637-5017(20)65446-1 (2020).
4. Colmone, A. et al. Leukemic cells create bone marrow niches that disrupt the behavior of normal hematopoietic progenitor cells. *Science* **322**, 1861–1865 (2008).
5. Ayala, F., Dewar, R., Kieran, M. & Kalluri, R. Contribution of bone microenvironment to leukemogenesis and leukemia progression. *Leukemia* **23**, 2233–2241 (2009).
6. Hurwitz, S. N., Jung, S. K. & Kurre, P. Hematopoietic stem, and progenitor cell signaling in the niche. *Leukemia* **34**, 3136–3148 (2020).
7. Alhaj Hussen, K. et al. Molecular and functional characterization of lymphoid progenitor subsets reveals a bipartite architecture of human lymphopoiesis. *Immunity* **47**, 680–696.e8 (2017) .
8. Francis, O. L., Milford, T. A., Beldiman, C. & Payne, K. J. Fine-tuning patient-derived xenograft models for precision medicine approaches in leukemia. *J. Invest. Med*. **64**, 740–744 (2016).
9. Subramanian, A. et al. Gene set enrichment analysis: a knowledge-based approach for interpreting genome-wide expression profiles. *Proc. Natl Acad. Sci. USA* **102**, 15545–15550 (2005).
10. Enciso, J., Mendoza, L. & Pelayo, R. Normal vs. malignant hematopoiesis: the complexity of acute leukemia through systems biology. *Front. Genet*. **6**, 290 (2015).

AUTHOR CONTRIBUTIONS

E.D.-P. and S.B. performed experiments collected and analyzed data. V.P., T.D.C.P., and M.S. performed experiments on NSG PDX mice and analyzed data. F.L. and B.S. performed RNA Seq and normalization of data, and B.S. and M.S. performed analysis. M.S. and C.D. designed the study and wrote the manuscript and provided financial support. C.D. provided patients samples and supervised the study. All authors approved the final manuscript as submitted and agree to be accountable for all aspects of the work.

FUNDING

The project was supported by "Les Hospices Civils de Lyon", "La Ligue contre le Cancer" (Comité Départementale de l'Ain), the association "Regarde chaque jour le Monde", the association "Le 111 des Arts", and "L'association pour la recherche contre le cancer" (ARC). The authors have no financial relationships relevant to this article to disclose.

COMPETING INTERESTS

The authors declare no competng interests.

CONSENT STATEMENT

The consent of the parental authority was systematically obtained before each sample collection. This study was validated by the ethics committee of the Hospices Civils de Lyon (Lyon, France), and was registered under the number: Clinicaltrials.gov: NCT03278145.

ADDITIONAL INFORMATION

Correspondence and requests for materials should be addressed to Carine Domenech.